Danger-associated peptide signaling in *Arabidopsis* requires clathrin

Fausto Andres Ortiz-Morea[a,b,c,d], Daniel V. Savatin[a,b], Wim Dejonghe[a,b], Rahul Kumar[a,b,1], Yu Luo[a,b,2], Maciej Adamowski[e], Jos Van den Begin[f], Keini Dressano[c], Guilherme Pereira de Oliveira[a,b], Xiuyang Zhao[a,b], Qing Lu[a,b], Annemieke Madder[f], Jiří Friml[e], Daniel Scherer de Moura[c], and Eugenia Russinova[a,b,3]

[a]Department of Plant Systems Biology, VIB, 9052 Ghent, Belgium; [b]Department of Plant Biotechnology and Bioinformatics, Ghent University, 9052 Ghent, Belgium; [c]Laboratory of Molecular and Plant Biology, Department of Genetics, College of Agriculture, University of São Paulo, Piracicaba, SP 13418-900, Brazil; [d]Agricultural Engineering Program, University of the Amazon, Florencia 180002622, Colombia; [e]Institute of Science and Technology Austria, 3400 Klosterneuburg, Austria; and [f]Laboratory for Organic and Biomimetic Chemistry, Department of Organic Chemistry, Ghent University, 9000 Gent, Belgium

Edited by Natasha V. Raikhel, Center for Plant Cell Biology, Riverside, CA, and approved July 29, 2016 (received for review April 15, 2016)

The *Arabidopsis thaliana* endogenous elicitor peptides (*At*Peps) are released into the apoplast after cellular damage caused by pathogens or wounding to induce innate immunity by direct binding to the membrane-localized leucine-rich repeat receptor kinases, PEP RECEPTOR1 (PEPR1) and PEPR2. Although the PEPR-mediated signaling components and responses have been studied extensively, the contributions of the subcellular localization and dynamics of the active PEPRs remain largely unknown. We used live-cell imaging of the fluorescently labeled and bioactive pep1 to visualize the intracellular behavior of the PEPRs in the *Arabidopsis* root meristem. We found that *At*Pep1 decorated the plasma membrane (PM) in a receptor-dependent manner and cointernalized with PEPRs. Trafficking of the *At*Pep1-PEPR1 complexes to the vacuole required neither the *trans*-Golgi network/early endosome (TGN/EE)-localized vacuolar H^+-ATPase activity nor the function of the brefeldin A-sensitive ADP-ribosylation factor-guanine exchange factors (ARF-GEFs). In addition, *At*Pep1 and different TGN/EE markers colocalized only rarely, implying that the intracellular route of this receptor–ligand pair is largely independent of the TGN/EE. Inducible overexpression of the *Arabidopsis* clathrin coat disassembly factor, *Auxilin2*, which inhibits clathrin-mediated endocytosis (CME), impaired the *At*Pep1-PEPR1 internalization and compromised *At*Pep1-mediated responses. Our results show that clathrin function at the PM is required to induce plant defense responses, likely through CME of cell surface-located signaling components.

Arabidopsis | clathrin | endogenous peptides | PEPR | endocytosis

Danger- or damage-associated molecular patterns (DAMPs) are diverse endogenous molecules that originate from the host to activate immune responses following perception (1). In *Arabidopsis*, the endogenous elicitor peptides, *At*Peps, are characterized as DAMPs because they are able to trigger defense responses reminiscent of those induced in pattern-triggered immunity (2, 3). *At*Peps form a family of eight members that mature from their precursor proteins PROPEP1 to PROPEP8. Because *At*Peps are induced by pathogen-associated molecular patterns and can induce their own transcription, they are also considered defense response amplifiers (4). All *At*Peps are perceived by two homologous leucine-rich repeat (LRR) pattern recognition receptors, PEP RECEPTOR1 (PEPR1) and PEPR2, but early studies implicated PEPR1 as the primary receptor for *At*Pep1 (2, 4, 5). *At*Pep1 is a 23-aa peptide derived from the C terminus of a 92-aa precursor protein, *At*PROPEP1 (3, 6). The 10 C-terminal amino acids of *At*Pep1 bind the PEPR1-LRR domain and trigger interaction between PEPR1 and its coreceptor, BRASSINOSTEROID INSENSITIVE1-ASSOCIATED KINASE1 (BAK1) (5). Despite the ever-growing number of plant signaling peptides, their intracellular dynamics have not been reported to date. PEPRs are structurally similar to the plasma membrane (PM)-localized receptor kinases FLAGELLIN SENSING2 (FLS2) and BRASSINOSTEROID INSENSITIVE1 (BRI1), which undergo endocytosis both independently and dependently of their ligands, the bacterial peptide flagellin 22 (flg22) and the brassinosteroid (BR) hormone, respectively (7, 8).

Endocytosis is proposed to function as a spatial and temporal modulator of the outcome of receptor-mediated responses by regulating the amounts of the respective receptors and ligands at the PM and their localization into the cell (9). In plants, clathrin-mediated endocytosis (CME) is the major internalization route (10). Functional studies of mutants in the clathrin machinery support the conserved mechanism of CME in plants and its importance for growth, development, and plant defense responses (11, 12), although, in general, the role of CME in plant immunity has not been addressed completely.

Here we used live-cell imaging of the fluorescently labeled pep1 (TAMRA-pep1) to study the contributions of the subcellular localization and dynamics of the active PEPRs to *At*Pep1 responses. We found that *At*Pep1-PEPR1 complexes are internalized via CME and transported to the vacuole via a *trans*-Golgi network/early endosome (TGN/EE)-independent pathway. We show that impaired clathrin function compromised the *At*Pep1 responses, indicating that clathrin plays a positive role in danger-associated peptide signaling in *Arabidopsis*.

Significance

Plant endogenous molecules, such as the *Arabidopsis thaliana* elicitor peptides (*At*Peps), activate defense responses by means of cell surface-located receptors that serve as an excellent model to study the implications of endomembrane trafficking in plant immunity. Here we used fluorescently labeled and bioactive pep1 to probe in vivo the intracellular dynamics and the fate of the active receptor-ligand complexes in the *Arabidopsis* root meristem. We show that *At*Pep1 internalization depends on its receptors and that clathrin-mediated endocytosis is essential for *At*Pep1-induced responses.

Author contributions: F.A.O.-M., J.F., D.S.d.M., and E.R. designed research; F.A.O.-M., D.V.S., W.D., R.K., Y.L., M.A., J.V.d.B., K.D., G.P.d.O., X.Z., Q.L., and A.M. performed research; F.A.O.-M., A.M., J.F., D.S.d.M., and E.R. analyzed data; and F.A.O.-M. and E.R. wrote the paper.

The authors declare no conflict of interest.

This article is a PNAS Direct Submission.

See Commentary on page 10745.

[1]Present address: Department of Plant Sciences, School of Life Sciences, University of Hyderabad, Telangana 500046, India.

[2]Present address: State Key Laboratory of Molecular and Developmental Biology, Institute of Genetics and Developmental Biology, Chinese Academy of Sciences, Beijing 100101, China.

[3]To whom correspondence should be addressed. Email: eurus@psb.vib-ugent.be.

This article contains supporting information online at www.pnas.org/lookup/suppl/doi:10.1073/pnas.1605588113/-/DCSupplemental.

Results

***At*Pep1 Labeled the PM of *Arabidopsis* Root Meristem Cells in a Receptor-Dependent Manner.** To simultaneously monitor the localization of the *At*Pep1-bound and presumably active PEPRs in living cells, we synthesized a fluorescently labeled *At*Pep1, designated TAMRA-pep1. When applied to plants, TAMRA-pep1 was stable (Fig. S1) and biologically active at nanomolar concentrations, as evaluated by different readouts for *At*Pep1 responses (Fig. S2). The localization of the labeled peptide was studied in epidermal cells of the root meristem of 5-d-old wild type (WT) *Arabidopsis* seedlings incubated with 100 nM TAMRA-pep1 for different time points and visualized immediately after three washouts (Fig. S3*A*). Incubation with TAMRA-pep1 for 60 s was sufficient to label all cells in the root meristem (Fig. 1*A*); however, previous promoter-β-glucoronidase (*GUS*) reporter studies of the *PEPR1* and *PEPR2* genes in *Arabidopsis* have shown that the two receptors are expressed in leaves and in the root differentiation zone, but not in the root meristem (6), in agreement with our results (Fig. S4*A*).

Because TAMRA-pep1 efficiently labeled the PM of root meristem cells, we wanted to clarify this discrepancy in localization patterns. Therefore, we expressed the genomic sequences of *PEPR1* and *PEPR2* fused to GFP under their native promoters into the *pepr1pepr2* double mutant and evaluated their expression patterns in the root meristem. The two chimeric proteins, PEPR1-GFP and PEPR2-GFP, were functional, because they complemented the *pepr1pepr2* double mutant (Fig. S4*B*). Whereas the expression pattern of the PEPR2-GFP protein was similar to that of the *pPEPR2::NLS-GFP* fusion, the PEPR1-GFP signal was detected in root cells of the differentiation zone and also in the root meristem, in correlation with the TAMRA-pep1 localization (Fig. 1*B* and Fig. S4*C*).

The PM labeling by TAMRA-pep1 in the root meristem depended on the receptors, as demonstrated by the finding that root cells of the *pepr1pepr2* double mutant lacked fluorescent labeling despite functional endocytosis (Fig. 1*C* and Fig. S3 *A* and *B*). This observation was further supported by a competition experiment in which pretreatment with a 10-fold excess of unlabeled pep1 prevented PM labeling by TAMRA-pep1, whereas labeling was unaffected by pretreatment with flg22, known to bind and activate the LRR receptor kinase FLS2 (7) (Fig. 1*D* and Fig. S3*C*).

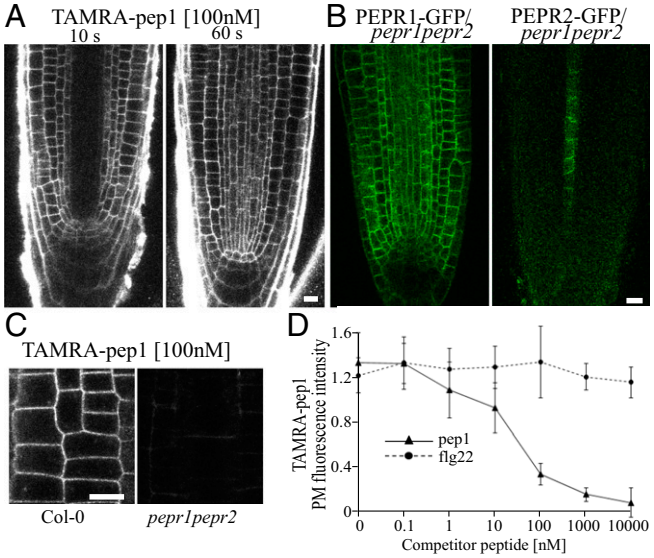

Fig. 1. PEPR-dependent PM labeling of TAMRA-pep1. (*A*) Root tips of *Arabidopsis* Col-0 seedlings treated with TAMRA-pep1 (100 nM, for 10 s and 60 s) and imaged after three washouts. (*B*) Localization of PEPR1-GFP and PEPR2-GFP expressed under endogenous promoters and complementing the *pepr1pepr2* double mutant. (*C*) Unlabeled PM of the *pepr1perp2* double mutant by TAMRA-pep1. Root epidermal cells were treated with TAMRA-pep1 for 60 s and imaged as in *A*. (*D*) Quantification of TAMRA-pep1 PM fluorescence intensity in root epidermal cells ($n = 48$) incubated with different concentrations of pep1 or flg22 for 5 min, then treated with TAMRA-pep1 (100 nM, 10 s) and imaged after three washouts (Fig. S3*C*). All experiments were performed using 5-d-old seedlings. Error bars indicate SD. *n*, number of cells. (Scale bars: 10 μm.)

Receptor-Mediated Endocytosis *of At*Pep1. To monitor the behavior of the bioactive fluorescently labeled pep1 over time, *Arabidopsis* seedlings were pulsed with TAMRA-pep1 (100 nM, 10 s), washed, and imaged at different time points (referred to as chases) (Fig. S5*A*). After a 10-min chase, most of the TAMRA fluorescence was associated with the PM. Some puncta were visible inside the cell after a 20-min chase and became more evident after a 40-min chase. Later, after a 90-min chase, TAMRA-pep1 was concentrated into structures that resembled vacuoles likely undergoing degradation (Fig. S5*A*). The TAMRA-pep1 internalization depended on the temperature (Fig. S3*D*).

To investigate whether PEPR1 and PEPR2 are also internalized after stimulation with pep1, we used *pepr1pepr2 Arabidopsis* plants complemented with *pRPS5A::PEPR1-GFP* or *pRPS5A::PEPR2-GFP* to allow robust expression of both receptors in the root meristem cells (Fig. S4*B*). The subcellular localization of PEPR1-GFP was evaluated after treatment with different pep1 concentrations after 5-min and 40-min chases (Fig. S5*B*). Although some PEPR1-GFP–labeled intracellular puncta were detected even without pep1 treatment, their presence was induced by pep1 in a time- and dose-dependent manner and was largely colocalized with the endocytic tracer FM4-64 (10) (Fig. S6*A*).

To determine whether the PEPR1 internalization followed similar TAMRA-pep1 dynamics, pRPS5A::PEPR1-GFP/*pepr1pepr2* seedlings were pulsed with pep1 (100 nM, 10 s) and imaged over time. Comparable to TAMRA-pep1, the PEPR1-GFP signal was first associated with the PM (10-min chase); later (20-min chase), punctate vesicle-like structures began to appear and became more abundant after a 40-min chase. At later time points (90-min chase), PEPR1-GFP accumulated in the vacuole (Fig. S5*C*). In contrast, PEPR1-GFP remained localized in the PM after treatment with flg22 (Fig. S5*B*), suggesting that the PEPR1 internalization is specifically induced by its ligand. The temporal dynamics of the PEPR1-GFP internalization after continuous application of pep1 remained the same as after the 10-s pulse (Fig. S5*D*).

To study the subcellular dynamics of *At*Pep1-PEPRs, ligand-receptor complexes in root meristem epidermal cells of pRPS5A::PEPR1-GFP/*pepr1pepr2* and pRPS5A::PEPR2-GFP/*pepr1pepr2* seedlings were pulsed with TAMRA-pep1 (100 nM, 10 s) and imaged after washout. TAMRA-pep1 and PEPR1-GFP and PEPR2-GFP cointernalized with the same temporal dynamics (Fig. 2 and Fig. S6*B*) as previously shown individually for TAMRA-pep1 and PEPR1-GFP. High Pearson's correlation coefficient values were obtained when TAMRA-pep1 colocalized with either PEPR1-GFP or PEPR2-GFP; thus, our observations are consistent with the view of a receptor-mediated *At*Pep1 internalization.

The *At*Pep1-PEPR Trafficking Is Largely Independent of V-ATPase Activity at the TGN/EE. To better understand the endocytic route of PEPR with its ligand, we incubated various fluorescence-tagged endomembrane markers with TAMRA-pep1 and assessed their colocalization after a 40-min chase by counting as positive only the vesicles with colocalization values >0.5 calculated by Pearson's correlation coefficient. TAMRA-pep1 colocalized only partially (18–37%) with all tested TGN markers, including VHA-a1, SYP61, SYP42, clathrin, and YFP-RabA1e (13–17) (Fig. S7*A*). TAMRA-pep1 colabeled only 5% of the Golgi SNARE, MEMB12 (17) and 3.4% of the autophagy marker ATG8 (Fig. S7 *B* and *C*). In addition, TAMRA-pep1

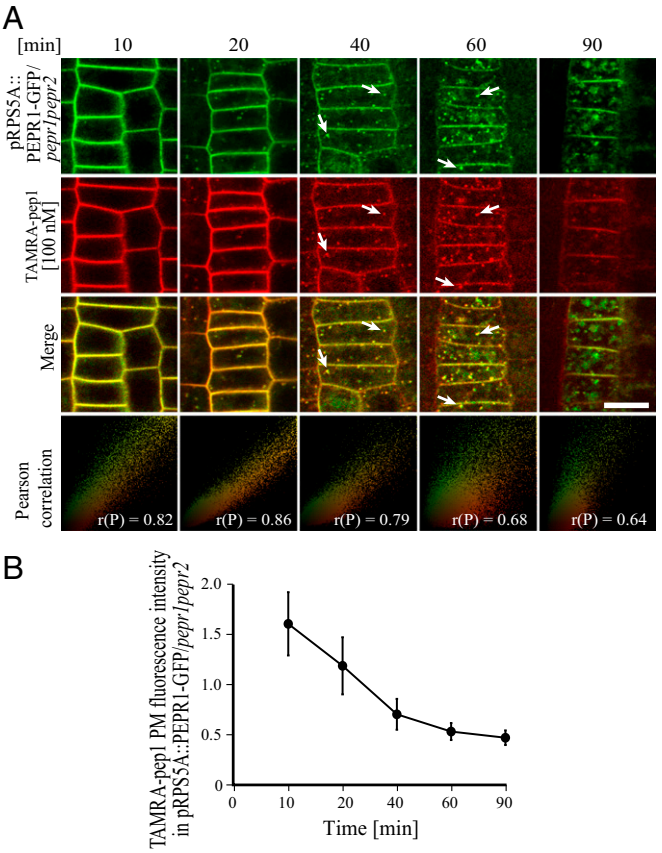

Fig. 2. Internalization of *At*Pep1 and its receptor PEPR1. (*A*) Here 5-d-old *pepr1pepr2* seedlings complemented with the pRPS5A::PEPR1-GFP construct were treated with TAMRA-pep1 for 10 s, washed with medium three times, and imaged at the indicated times. As a colocalization indicator, the Pearson correlation (*P*) was calculated for merged images. White arrows point to colocalized structures. (Scale bars: 10 μm.) (*B*) Quantification of PEPR1-GFP PM fluorescence intensity in *A* ($n = 27$). *n*, number of cells analyzed. Error bars indicate SD.

uptake was not affected in different autophagy mutants (Fig. S7*D*). In contrast, colocalization increased (76–84%) between TAMRA-pep1 and the multivesicular body (MVB) markers ARA7 and ARA6 (17, 18) (Fig. S7*E*). Finally, TAMRA-pep1 accumulated in the vacuoles marked by VAMP727 (17) (Fig. S7*F*). Taken together, the live-cell imaging analyses revealed that TAMRA-pep1 and, presumably, its bound receptors follow an endocytic trafficking route from the PM to the vacuole, passing through late endosomal compartments and, unexpectedly, only partially via the TGN/EEs or endomembranes neighboring it. This observation is in contrast to the BR receptor and its ligand that colabeled >80% of the TGN/EE compartments marked by the VHA-a1-RFP, as shown previously (8).

To support the colocalization studies, we investigated whether the trafficking route of the *At*Pep1-PEPR complexes requires the function of the vacuolar H^+-ATPase (V-ATPase), which is present in the TGN/EE compartments to acidify them (13). We examined the subcellular dynamics and localization of TAMRA-pep1 in transgenic lines expressing VHA-a1-GFP in the presence of the specific V-ATPase inhibitor concanamycin A (ConcA) (13) (Fig. 3*A*). Surprisingly, after a 40-min chase, the fluorescent probe did not accumulate in typical ConcA bodies, as seen for the VHA-a1-GFP, despite some minor colocalization. After a 90-min chase, the TAMRA-pep1 signal was visible in the vacuole, indicating that its trafficking, although somewhat delayed (Fig. S8*A*), was not blocked by the inhibition of the V-ATPase activity. These findings are supported by the subcellular dynamics of PEPR1-GFP in the presence of ConcA and the endosomal tracer FM4-64, previously shown to accumulate into the TGN/EE-positive ConcA bodies (13) (Fig. 3*B*). For this experiment, pRPS5A::PEPR1-GFP/*pepr1pepr2* seedlings were pretreated with ConcA (2 μM, 30 min), then pulsed with pep1 or with water (mock control), in the presence of FM4-64 and ConcA. Seedlings stained with FM4-64 pretreated and treated with DMSO were used as a control for the ConcA treatment. Without pep1 elicitation, PEPR1-GFP localization was not significantly affected by ConcA, although at later points

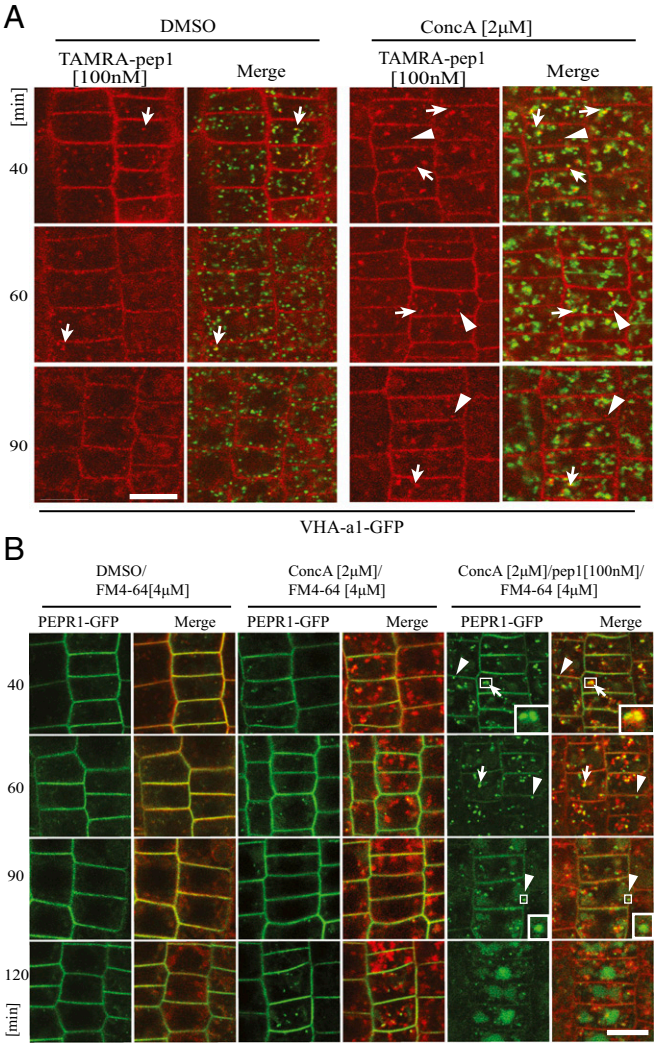

Fig. 3. The trafficking of TAMRA-pep1 and PEPR1-GFP to the vacuole did not require V-ATPase activity. (*A*) Subcellular localization of TAMRA-pep1 in *Arabidopsis* root meristem epidermis of transgenic seedlings expressing the TGN/EE marker VHA-a1-GFP in the presence of ConcA and DMSO (mock control) over time. Seedlings were pretreated with ConcA (2 μM, 30 min) and then with TAMRA-pep1 (100 nM, 10-s pulse, three washouts) in the presence of ConcA (2 μM) for 40, 60, and 90 min before imaging. Arrows and arrowheads point to colocalized and uncolocalized vesicles marked with TAMRA-pep1 and VHA-a1-GFP, respectively. (*B*) Subcellular localization of PEPR1-GFP in *Arabidopsis* root epidermal meristem cells in the presence of DMSO, ConcA (2 μM), and ConcA (2 μM)/pep1 (100 nM for 10 s) over time. *pepr1pepr2* seedlings complemented with the pRPS5A::PEPR1-GFP construct were pretreated with ConcA (2 μM, 30 min) and then exposed or not to pep1, stained with FM4-64 (4 μM, 5 min, three washouts), and kept in the presence of ConcA (2 μM) for the indicated times until imaging. Arrows and arrowheads point to PEPR1-GFP vesicles colocalized and uncolocalized with FM4-64, respectively. (*Insets*) 3× magnification showing details of the PEPR1-GFP vesicles. In all experiments, 5-d-old seedlings were used. (Scale bars: 10 μm.)

some GFP-positive compartments were seen either in the proximity of or colocalizing with the FM4-64–positive ConcA bodies (Fig. 3*B*). After pretreatment with ConcA and pep1 application in the presence of the inhibitor, a considerable portion of PEPR1-GFP–marked vesicles clearly colocalized with FM4-64 into the ConcA bodies and were still better visualized after 40- and 60-min chases (Fig. 3*B*), but, as seen for TAMRA-pep1 (Fig. 3*A*), the PEPR1-GFP trafficking to the vacuoles was not blocked. Based on the low colocalization between TAMRA-pep1 and VHA-a1-GFP and the ineffectiveness of ConcA, we concluded that trafficking of the *At*Pep1-PEPR complexes to the vacuole does not strictly require the V-ATPase activity associated with TGN/EE.

PEPR1 Secretion, but Not Its Endocytosis, Depends on ARF-GEF. Most of the plant PM proteins, including receptors, constitutively cycle between PM and endosomal compartments, a mechanism that modulates their abundance and activity (19). Therefore, to investigate whether PEPR1 also undergoes recycling, we applied the fungal inhibitor brefeldin A (BFA), which is also routinely used to block recycling in plants through inhibition of the BFA-sensitive ADP-ribosylation factor-guanine exchange factors (ARF-GEFs) (20). Following treatment with BFA (50 μM, 60 min), PEPR1-GFP fluorescence clearly accumulated in BFA bodies that were also costained with the endocytic tracer FM4-64 (Fig. 4 *A* and *B*). Because PEPR-GFP did not accumulate into BFA bodies in the presence of BFA and the protein synthesis inhibitor cycloheximide (CHX) (Fig. 4*C*), we concluded that the majority of the PEPR1-fluorescent signals that accumulated in the BFA bodies without CHX belonged to newly synthetized, but not recycled, PEPR1 proteins.

Next, we visualized PEPR1-GFP fluorescence after 40- and 60-min chases following *At*Pep1 elicitation in the presence of BFA (50 μM) (Fig. 4*D*). After a 40-min chase, the PEPR1-GFP fluorescence accumulated into BFA bodies (likely derived from secretion) and into a population of vesicles arranged around the BFA bodies, some of which seemed to colocalize with the BFA bodies (Fig. 4*D*, *Inset*). After a 60-min chase, the PEPR1-GFP fluorescent signal was also seen in the vacuole, indicating that the ligand-induced internalization of PEPR1 was not blocked. To confirm this observation, we evaluated the internalization of TAMRA-pep1 in the presence of BFA (Fig. 4*E*). The treatment was performed in transgenic plants expressing the endosomal marker VHA-a1-GFP, which has been detected in the core of BFA bodies (13). As expected, the localization pattern and temporal dynamics of TAMRA-pep1 in the presence of BFA were similar to those of PEPR1-GFP after activation (Fig. 4*E*). These observations suggest that the endocytic trafficking of *At*Pep1-PEPR complexes is not compromised in the presence of BFA, as previously reported for FLS2 in *Arabidopsis* leaves (7).

Clathrin Is Required for *At*Pep1-PEPR1 Complex Internalization and *At*Pep1 Responses. In plants, CME is the major internalization route of plant PM proteins (10). To gain further insight into the internalization mechanism of *At*Pep1-PEPR complexes, we characterized TAMRA-pep1 endocytosis in the *clathrin heavy chain 2* (*chc2*) knockout mutants (*chc2-1* and *chc2-2*) (11). In both *chc2* alleles, the intracellular accumulation of TAMRA-pep1 was slightly, but significantly, reduced, implying its impaired internalization (Fig. S8 *B* and *C*). To corroborate these observations, we took advantage of the inducible line expressing the clathrin-interacting protein Auxilin2 (AX2) (XVE>>AX2), the overexpression of which blocked CME in *Arabidopsis* (Fig. 5*A*). When seedlings were induced with 5 μM estradiol, monitored as root growth arrest, both the internalization of TAMRA-pep1 and FM4-64 were completely blocked, suggesting that the *At*Pep1-PEPR complexes undergo CME.

To investigate whether the internalization of *At*Pep1-PEPR requires the known CME adaptor AP-2, we also carried out TAMRA-pep1 uptake experiments in root epidermal cells of

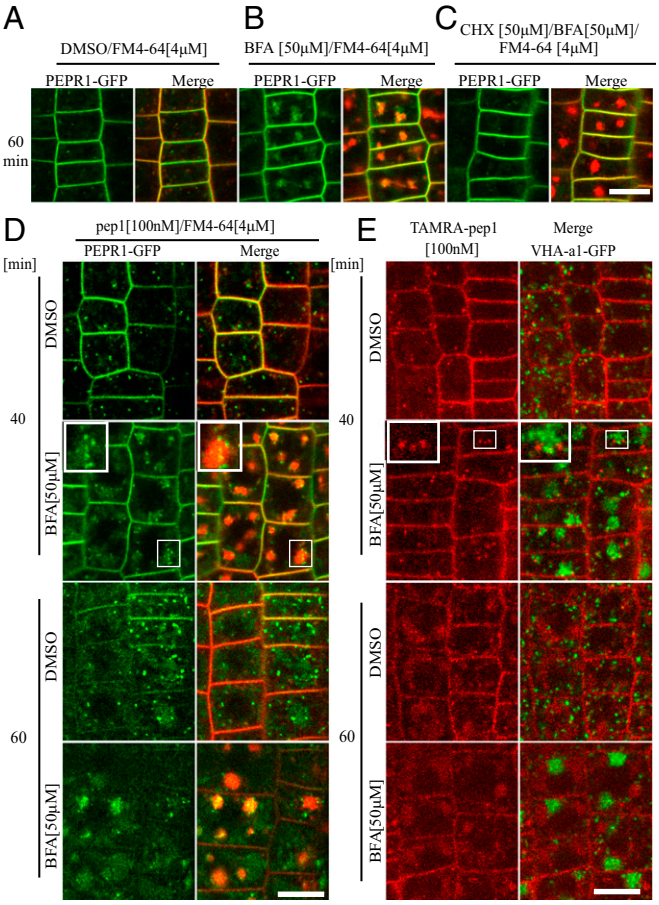

Fig. 4. PEPR1 secretion, but not its endocytosis, depends on ARF-GEF. (*A*–*C*) Subcellular localization of PEPR1-GFP after treatment for 60 min with DMSO (*A*), BFA (50 μM) (*B*), and CHX (50 μM) + BFA (50 μM) (*C*). (*D*) Experiments performed after pretreatment with CHX for 1 h. Subcellular localization of PEPR1-GFP after 40 and 60 min of pep1 elicitation (100 nM, 10-s pulse) in the presence or absence of BFA (50 μM). *pepr1pepr2* seedlings complemented with the pRPS5A::PEPR1-GFP construct were stained with FM4-64 (4 μM, 5 min, three washouts). (*E*) Subcellular localization of TAMRA-pep1 in the presence or absence of BFA. Seedlings expressing VHA-a1-GFP were treated with TAMRA-pep1 for 10 s, washed, kept in the presence or absence of BFA (50 μM), and imaged after 40 and 60 min. (*Insets*) Details of BFA bodies at 2.5× magnification. In all experiments, 5-d-old seedlings were used. (Scale bars: 10 μm.)

ap2m-2 (21) and *ap2s* (22) mutants defective in the medium and small subunits of the *Arabidopsis* AP-2, respectively (Fig. S8 *B* and *C*). Notably, the uptake of TAMRA-pep1 was not significantly compromised in any of these lines, in contrast to the previously reported, partially inhibited FM4-64 uptake (22, 23).

We next tested whether CME impairment would affect early and late *At*Pep1 responses, including mitogen-activated protein kinase (MAPK) activation and root growth inhibition, respectively (12). Although the MAPK phosphorylation caused by pep1 application was not affected in any of the tested *chc2*, *ap2m*, and *ap2s* alleles (Fig. S9), it was strongly reduced when XVE>>AX2 seedlings were induced for 24 h with estradiol and treated with pep1 (Fig. 5*B*). Interestingly, the root sensitivity of the *chc2* mutants to pep1 application was also altered, but only at one pep1 concentration (Fig. S8*D*). To rule out the possibility that the reduced MAPK activation was not due to impaired secretion, we checked the amount of PEPR1-GFP receptors and the TAMRA-pep1 available at the PM by measuring the fluorescence intensity before and after estradiol induction in XVE>>AX2 seedlings. We observed a PM-localized receptor and, in some cases, even an

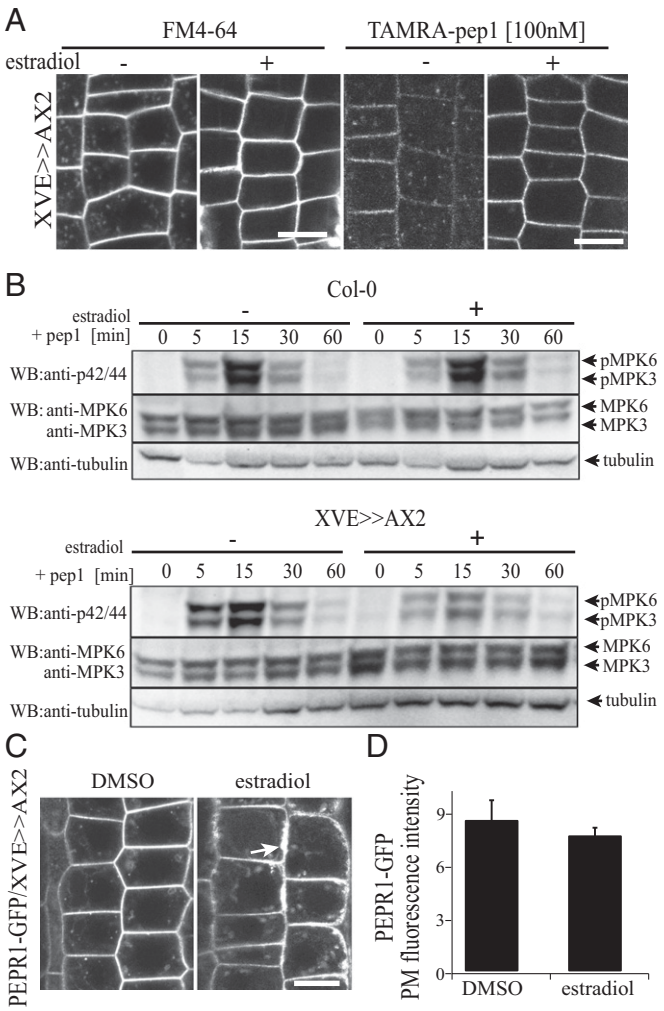

Fig. 5. Clathrin dependence of *At*Pep1-PEPR internalization and responses. (*A*) The internalization of FM4-64 (*Left*; 4 μM, 5 min, three washouts, 30-min chase) and TAMRA-pep1 (*Right*; 100 nM, 10-s pulse, three washouts, 40-min chase) was blocked after induction of *Auxilin2 (AX2)* expression in 5-d-old XVE>>AX2 seedlings with 5 μM estradiol for 24 h. (*B*) Pep1-induced (20 nM) MAPK activation was impaired after the XVE>>AX2 line had been treated with 5 μM estradiol for 24 h. Phosphorylation of MPK6 and MPK3 was detected with anti–phospho-p44/p42-MPK antibody. The blot was reprobed with anti-MPK6, ant-MPK3, and anti-tubulin to show protein levels. Individual MPKs were identified by molecular mass and are indicated by arrows. These experiments were repeated five times. (*C*) Subcellular localization of PEPR1-GFP in root epidermal cells of *pRPS5A::PEPR1-GFP/XVE>>AX2*-expressing seedlings before (DMSO) and after induction with 5 μM estradiol for 24 h. (*D*) Quantification of PEPR1-GFP PM fluorescence intensity in *C* ($n = 36$). n, number of cells analyzed. Error bars indicate SEM. No statistically significant difference (*$P \leq 0.01$, Student's *t* test) was found. (Scale bars: 10 μm.)

excessive amount of membranous material that accumulated at the periphery of epidermal cells, suggesting that secretion was not blocked (Fig. 5 *C* and *D*). Complementary to these results, MAPK activation after pep1 application was not compromised in mutants in the AP1M subunit of the TGN/EE-localized AP-1 complex, which is essential for post-Golgi trafficking (24) (Fig. S9 *A* and *B*). Based on the foregoing findings, we conclude that clathrin is required for *At*Pep1-PEPR–mediated responses through CME regulation.

Discussion

Here we used live-cell imaging of fluorescently labeled and biologically active pep1 (TAMRA-pep1) to assess the importance of the subcellular localization and dynamics of the *At*Pep-PEPR complexes for signaling in the root meristem. TAMRA-pep1 associated rapidly and in a receptor-dependent manner with the PM, in agreement with previous biochemical work showing that receptor-ligand complexes are formed within seconds (5). The TAMRA-pep1 localization correlated with the expression pattern of the PEPR1-GFP protein. TAMRA-pep1 and PEPR-GFP were simultaneously internalized and transported to the vacuole, most probably as a mechanism to desensitize cells after the *At*Pep1 stimulation, as reported for other ligands (8, 25). Interestingly, the temporal dynamics of the *At*Pep1-PEPR complexes differed from those of BR-BRI1, which internalize very rapidly (8), but were similar to those of the FLS2 receptor (7). Thus, diverse signaling responses require endocytosis with different dynamics and, notably, pattern recognition receptors follow ligand-induced endosomal trafficking with similar dynamics.

Because TGN/EE is the first compartment that gathers endocytosed cargos (26), high colabeling was expected between the TGN/EE markers and TAMRA-pep1, as previously observed for the BRI1 receptor-ligand complexes (8). Surprisingly, and similar to FLS2 (7, 27), the colocalization of TAMRA-pep1 with all tested TGN/EE markers, including clathrin (28) and VHA-a1, was low, in contrast to the MVB markers, for which high colocalization values were obtained. Possibly, the *At*Pep1-PEPR complexes either are internalized directly to MVBs bypassing the TGN/EE or are transported to the MVBs via a V-ATPase–negative subpopulation of the TGN. In agreement, the transport of TAMRA-pep1 to the vacuole, although delayed, was not blocked by the inhibitor of the V-ATPase activity, ConcA (13), similarly to the boron transporter BOR1 at high boron concentrations (29) and the FLS2 receptor (7, 27). Intriguingly, ARA7 colocalized with the VHA-a1 in the TGN/EE, thus marking the TGN/EE subdomains that will mature into MVBs (30). Therefore, PEPRs might associate with TGN/EE subpopulations that are partially excluded from the V-ATPase activity preceding the switch to ARA7-dependent TGN/EE maturation into MVBs. The identity of this TGN subpopulation remains to be determined, however. The fungal toxin BFA induced the accumulation of the inactive PEPR1-GFP into BFA bodies, but these bodies were not detected after protein synthesis inhibition, implying that the signal detected in BFA bodies derives from secreted, instead of recycled, receptors.

Although we cannot rule out a BFA-insensitive recycling pathway or a very slow recycling rate, our results suggest that the abundance of the inactive receptors at the PM is regulated mainly by secretion. Because PEPRs function as innate immunity amplifiers and their expression is also induced by *At*Peps (4), we can predict that after elicitation the internalized PEPRs are replaced by newly synthetized proteins. Accordingly, BFA did not affect the *At*Pep1-PEPR1 trafficking to the vacuole, as previously reported for the activated FLS2 receptor and the fluorescent BR analog (7, 8).

Direct evidence for the role of CME in plant endogenous peptide-mediated responses has not yet been reported. We have shown that the endocytosis of *At*Pep1-PEPR1 depends on clathrin, because TAMRA-pep1 internalization was slightly reduced in *chc2* alleles and completely blocked after overexpression of the clathrin-interacting protein AX2 that seemingly prevents clathrin recruitment to the nascent endocytic pits. The inhibition of TAMRA-pep1 internalization after overexpression of *AX2* correlated with severely reduced activation of MAPKs after pep1 application. In agreement, in response to pep1, the root growth insensitivity of the two *chc2* alleles was increased but, surprisingly, at only one pep1 concentration. Taken together, our results reveal that *At*Pep1-mediated responses are compromised and that the severity of the phenotypes, at least related to early MAPK responses, correlates with the extent of the CME inhibition at the PM.

In plants, clathrin-coated vesicles are also essential for sorting cargos for recycling and possibly secretion at the TGN/EE (28). Given that the amounts of PEPR1-GFP and TAMRA-pep1 at the PM were not reduced after AX2 induction, we conclude that the secretion of PEPR1 is not significantly affected. In addition, the *At*Pep1-mediated MAPK activation was not altered by mutations in the medium subunit of the TGN/EE-localized AP-1, which is essential for post-Golgi trafficking (24). Despite their involvement in CME, the mutant alleles of AP-2, *ap2m-2* and *ap2s* (21, 22), did not affect TAMRA-pep1 uptake or *At*Pep1-mediated MAPK activation, raising the question of whether PEPR endocytosis is mediated by AP-2.

Finally, in contrast to the BR signaling, clathrin is required for *At*Pep1-mediated responses. Whether CME is necessary for the delivery of signaling complexes to as-yet undefined endosomal compartments or for the removal of unknown negative *At*Pep1 signaling components from the PM remains to be determined.

Materials and Methods

The experimental procedures followed for this study are described in detail in *SI Materials and Methods*.

Plant Material and Growth Conditions. *Arabidopsis thaliana* (L.) Heynh. (Columbia accession, Col-0), *pepr1pepr2* (2), *chc2-1* and *chc2-2* (11), *ap1m2-1* and *hap13* (Ws) (24), *ap2m-2* (21), *ap2s* (22), *atg5-1* (31), and *atg7-2* (32) plants were used. Generation of constructs, used primers (Table S1), transgenic lines, media, and growth conditions are described in *SI Materials and Methods*.

Peptides. pep1 (ATKVKAKQRGKEKVSSGRPGQHN) and pep1 labeled with 5′-carboxytetramethylrhodamine (TAMRA-pep1) were purchased from Life Technologies. flg22 was acquired from Genscript. The peptides were dissolved in water to obtain peptide stocks of 100 μM. Details are provided in *SI Materials and Methods*.

Chemical Treatments. BFA (50 mM), ConcA (2 mM), and CHX (50 mM) were purchased from Sigma-Aldrich. FM4-64 (2 mM) was acquired from Molecular Probes. Here 5-d-old seedlings were incubated for the indicated times into 1 mL of growth medium containing 2 μM ConcA, 50 μM BFA, 50 μM CHX, or a combination of BFA and CHX. Details are provided in *SI Materials and Methods*.

Confocal Microscopy. *Arabidopsis* seedlings were imaged with an Olympus FluoView 1000 inverted confocal microscope or a Zeiss LSM 880 confocal laser scanning microscope. Details are provided in *SI Materials and Methods*.

ACKNOWLEDGMENTS. We thank D. Van Damme, E. Mylle, M. Castro Silva-Filho, and J. Goeman for providing useful advice and technical assistance; I. Hara-Nishimura, J. Lin, G. Jürgens, M. A. Johnson, and P. Bozhkov for sharing published materials; and M. Nowack and M. Fendrych for kindly donating the *pUBQ10::ATG8-YFP*-expressing marker line. F.A.O.-M. was supported by special research funding from the Flemish Government for a joint doctorate fellowship at Ghent University, and funding from the Student Program–Graduate Studies Plan Program from the Coordination for the Improvement of Higher Education Personnel, Brazil, for a doctorate fellowship at the University of São Paulo. X.Z. and Q.L. are indebted to the China Science Council and G.P.d.O. to the "Ciência sem Fronteiras" for predoctoral fellowships. R.K. and Y.L. have received postdoctoral fellowships from the Belgian Science Policy Office. This research was supported by Flanders Research Foundation Grant G008416N (to E.R.) and by the São Paulo Research Foundation and the National Council for Scientific and Technological Development (CNPq) (D.S.d.M.). D.S.d.M. is a research fellow of CNPq.

1. Endo S, Betsuyaku S, Fukuda H (2014) Endogenous peptide ligand-receptor systems for diverse signaling networks in plants. *Curr Opin Plant Biol* 21:140–146.
2. Krol E, et al. (2010) Perception of the *Arabidopsis* danger signal peptide 1 involves the pattern recognition receptor *At*PEPR1 and its close homologue *At*PEPR2. *J Biol Chem* 285(18):13471–13479.
3. Huffaker A, Pearce G, Ryan CA (2006) An endogenous peptide signal in *Arabidopsis* activates components of the innate immune response. *Proc Natl Acad Sci USA* 103(26): 10098–10103.
4. Yamaguchi Y, Huffaker A, Bryan AC, Tax FE, Ryan CA (2010) PEPR2 is a second receptor for the Pep1 and Pep2 peptides and contributes to defense responses in *Arabidopsis*. *Plant Cell* 22(2):508–522.
5. Tang J, et al. (2015) Structural basis for recognition of an endogenous peptide by the plant receptor kinase PEPR1. *Cell Res* 25(1):110–120.
6. Bartels S, et al. (2013) The family of Peps and their precursors in *Arabidopsis*: Differential expression and localization but similar induction of pattern-triggered immune responses. *J Exp Bot* 64(17):5309–5321.
7. Beck M, Zhou J, Faulkner C, MacLean D, Robatzek S (2012) Spatio-temporal cellular dynamics of the *Arabidopsis* flagellin receptor reveal activation status-dependent endosomal sorting. *Plant Cell* 24(10):4205–4219.
8. Irani NG, et al. (2012) Fluorescent castasterone reveals BRI1 signaling from the plasma membrane. *Nat Chem Biol* 8(6):583–589.
9. Sorkin A, von Zastrow M (2009) Endocytosis and signalling: Intertwining molecular networks. *Nat Rev Mol Cell Biol* 10(9):609–622.
10. Dhonukshe P, et al. (2007) Clathrin-mediated constitutive endocytosis of PIN auxin efflux carriers in *Arabidopsis*. *Curr Biol* 17(6):520–527.
11. Kitakura S, et al. (2011) Clathrin mediates endocytosis and polar distribution of PIN auxin transporters in *Arabidopsis*. *Plant Cell* 23(5):1920–1931.
12. Smith JM, et al. (2014) Loss of *Arabidopsis thaliana* Dynamin-Related Protein *2B* reveals separation of innate immune signaling pathways. *PLoS Pathog* 10(12):e1004578.
13. Dettmer J, Hong-Hermesdorf A, Stierhof Y-D, Schumacher K (2006) Vacuolar H^+-ATPase activity is required for endocytic and secretory trafficking in *Arabidopsis*. *Plant Cell* 18(3): 715–730.
14. Robert S, et al. (2008) Endosidin1 defines a compartment involved in endocytosis of the brassinosteroid receptor BRI1 and the auxin transporters PIN2 and AUX1. *Proc Natl Acad Sci USA* 105(24):8464–8469.
15. Uemura T, Suda Y, Ueda T, Nakano A (2014) Dynamic behavior of the *trans*-Golgi network in root tissues of Arabidopsis revealed by super-resolution live imaging. *Plant Cell Physiol* 55(4):694–703.
16. Dejonghe W, et al. (2016) Mitochondrial uncouplers inhibit clathrin-mediated endocytosis largely through cytoplasmic acidification. *Nat Commun* 7:11710.
17. Geldner N, et al. (2009) Rapid, combinatorial analysis of membrane compartments in intact plants with a multicolor marker set. *Plant J* 59(1):169–178.
18. Goh T, et al. (2007) VPS9a, the common activator for two distinct types of Rab5 GTPases, is essential for the development of *Arabidopsis thaliana*. *Plant Cell* 19(11): 3504–3515.
19. Kleine-Vehn J, Friml J (2008) Polar targeting and endocytic recycling in auxin-dependent plant development. *Annu Rev Cell Dev Biol* 24:447–473.
20. Naramoto S, et al. (2014) Insights into the localization and function of the membrane trafficking regulator GNOM ARF-GEF at the Golgi apparatus in *Arabidopsis*. *Plant Cell* 26(7):3062–3076.
21. Yamaoka S, et al. (2013) Identification and dynamics of *Arabidopsis* adaptor protein-2 complex and its involvement in floral organ development. *Plant Cell* 25(8):2958–2969.
22. Fan L, et al. (2013) Dynamic analysis of *Arabidopsis* AP2 σ subunit reveals a key role in clathrin-mediated endocytosis and plant development. *Development* 140(18): 3826–3837.
23. Bashline L, Li S, Anderson CT, Lei L, Gu Y (2013) The endocytosis of cellulose synthase in Arabidopsis is dependent on μ2, a clathrin-mediated endocytosis adaptin. *Plant Physiol* 163(1):150–160.
24. Park M, et al. (2013) *Arabidopsis* μ-adaptin subunit AP1M of adaptor protein complex 1 mediates late secretory and vacuolar traffic and is required for growth. *Proc Natl Acad Sci USA* 110(25):10318–10323.
25. Smith JM, Salamango DJ, Leslie ME, Collins CA, Heese A (2014) Sensitivity to Flg22 is modulated by ligand-induced degradation and de novo synthesis of the endogenous flagellin-receptor FLAGELLIN-SENSING2. *Plant Physiol* 164(1):440–454.
26. Viotti C, et al. (2010) Endocytic and secretory traffic in *Arabidopsis* merge in the trans-Golgi network/early endosome, an independent and highly dynamic organelle. *Plant Cell* 22(4):1344–1357.
27. Choi S-W, et al. (2013) RABA members act in distinct steps of subcellular trafficking of the FLAGELLIN SENSING2 receptor. *Plant Cell* 25(3):1174–1187.
28. Ito E, et al. (2012) Dynamic behavior of clathrin in *Arabidopsis thaliana* unveiled by live imaging. *Plant J* 69(2):204–216.
29. Takano J, Miwa K, Yuan L, von Wirén N, Fujiwara T (2005) Endocytosis and degradation of BOR1, a boron transporter of *Arabidopsis thaliana*, regulated by boron availability. *Proc Natl Acad Sci USA* 102(34):12276–12281.
30. Singh MK, et al. (2014) Protein delivery to vacuole requires SAND protein-dependent Rab GTPase conversion for MVB-vacuole fusion. *Curr Biol* 24(12):1383–1389.
31. Thompson AR, Doelling JH, Suttangkakul A, Vierstra RD (2005) Autophagic nutrient recycling in *Arabidopsis* directed by the ATG8 and ATG12 conjugation pathways. *Plant Physiol* 138(4):2097–2110.
32. Hofius D, et al. (2009) Autophagic components contribute to hypersensitive cell death in *Arabidopsis*. *Cell* 137(4):773–783.
33. Ebine K, et al. (2008) A SNARE complex unique to seed plants is required for protein storage vacuole biogenesis and seed development of *Arabidopsis thaliana*. *Plant Cell* 20(11):3006–3021.